THERMODYNAMIC LOW-ORDER MODEL FOR THE SIMULATION OF TWO-PHASE EXPANSION IN A TFC UNIT

Anastasios Skiadopoulos [1]*, Xander van Heule [2], George Kosmadakis [3], Dimitrios Manolakos [1], Michel De Paepe [2] and Steven Lecompte [2]

[1]Agricultural University of Athens, Department of Natural Resources and Agricultural Engineering, Athens, Attica, Greece

[2]Ghent University, Department of Electromechanical, Systems and Metal Engineering, Ghent, Belgium

[3]Ricreation IKE, Technological Park "Lefkippos", Agia Paraskevi, Attica, Greece

*Corresponding Author: tskiado@aua.gr

ABSTRACT

Numerical modeling of the two-phase expansion phenomenon may provide valuable tools for the evaluation of the efficiency of a Trilateral Flash Cycle (TFC) unit, as well as in the sizing and design optimization process of two-phase expanders. In the present work, a low-order thermodynamic model for the simulation of two-phase expansion in twin-screw expanders has been developed. The model simulates the phase change in the expansion chamber by discretizing it in a sufficient number of sub-chambers. At every sub-chamber, the energy and mass balance equations are solved for both liquid and gas phases, similar to a two-fluid model approach. The modeling procedure applies a lumped parameter approach, which requires the calculation of a set of parameters to provide a closure for the mass and energy balance of the expander under different operating conditions. The necessary set of parameters for the two-phase expansion in twin-screw expanders has been identified based on available experimental data. The values of the parameters have been calculated by solving a properly defined optimization problem. The results from the simulations indicate that the developed model can predict with satisfying accuracy the two-phase expansion along the expansion chamber.

1 INTRODUCTION

Currently, the state of the art technological solution for thermal energy recovery from low-grade heat sources is the Organic Rankine Cycle (ORC). However, the low thermal efficiency of the ORC in conjunction with the available potential for low-grade thermal energy recovery has attracted the interest of the scientific community in seeking methods for the improvement of the thermal efficiency of the ORC or in investigating the feasibility of different technological solutions.

The Trilateral Flash Cycle (TFC) power cycle seems to be one of the most promising alternatives to the ORC. The literature review indicates that the thermal efficiency and the power output of the TFC are very promising compared to other power cycles and variations of the ORC (Lecompte *et al.*, 2015; Iglesias Garcia *et al.*, 2018). In the TFC the expansion of the working fluid starts from the saturated liquid state, and the working fluid is a two-phase vapor-liquid mixture throughout the expansion process. Avoiding isothermal evaporation gives rise to an improved temperature match between the working fluid and the heat transfer fluid. Moreover, the exergy destruction during the evaporation process, inherent in the ORC, is avoided and, thus, the second law efficiency of the TFC can be superior. Despite the potential of the TFC, it has not been applied yet on a wide scale. Very few experimental works related to two-phase expansion have been published in the literature. Steidel *et al.* (1982) performed laboratory tests with geothermal fluids as a working fluid in a twin-screw expander with a maximum observed adiabatic efficiency equal to 53% for vapor quality between 8% and 27%. The work of Smith *et al.* (1996) with R113 as a working fluid in twin-screw expanders revealed that adiabatic efficiencies up to 80% are possible for the two-phase expansion. Kliem (2005) used water as the working fluid in twin-screw expanders with specially designed filling systems and indicated achievable adiabatic efficiency up to 50%. Mckay and Sprankle (1970) measured adiabatic efficiencies up to 62%

for a 1MW turbine for geothermal energy recovery and vapor qualities in the range 0-99%. Öhman and Lundqvist (2013) performed a series of laboratory tests in a semi-hermetic Lysholm turbine operating with R134a as a working fluid and superheated, saturated, and wet inlet gas conditions. Their tests revealed a maximum adiabatic efficiency of 92%. Kanno and Shikazono (2016) performed tests in a reciprocating cylinder mimicking a two-phase piston expander. Working fluids were water and ethanol and maximum achieved adiabatic efficiencies were 86% and 82% respectively.

Concerning the modeling of two-phase expansion, the literature survey indicates that currently there are no 3-D Computational Fluid Dynamics (CFD) simulations of two-phase expansion in volumetric expanders. However, a few lower-order models have been developed. Taniguchi *et al.* (1988) and Smith *et al.* (1996) developed analytical 1-D models for the simulation of two-phase expansion in twin-screw expanders. These models solve for the conservation of mass and energy in the expander, while the mixture is treated as a single fluid. An equation of state is used to correlate the thermodynamic properties of the working fluid. The vapor and liquid phases are assumed to be in thermodynamic equilibrium. Vasuthevan and Brümmer (2017) developed a thermodynamic 1-D model for the simulation of two-phase expansion in twin-screw expanders. The model solves for the liquid and vapor phases separately, and all calculations are performed with the assumption of thermodynamic equilibrium between phases. Lastly, Bianchi *et al.* (2020) developed a numerical model for the simulation of a twin-screw expander for low-grade heat recovery, wherein the two-phase mixture is treated as a single fluid and the Navier-Stokes equations along with the energy conservation equations are solved in a 1-D formulation.

In the present work, a semi-empirical low-order model for the simulation of two-phase expansion in twin-screw expanders has been developed. To the best of the authors' knowledge, this is the first work applying a semi-empirical approach to develop a numerical tool for the simulation of two-phase expansion. The selection of the volumetric expander type for the model development was based on the fact that twin-screw expanders have been proven to be suitable for power generation in the range of tens to a few hundreds of kWs, a power range typical in low-grade heat recovery (Bianchi *et al.*, 2018). Moreover, they are capable to handle two-phase vapor-liquid flows and large mass flow rates which are anticipated in TFC systems because the working fluid remains in the saturated liquid state after heat has been transferred to the system. The methodological background for the numerical procedure is based on the work of Lemort *et al.* (2009). The key concept is the identification of a set of unknown parameters which provide a closure for the governing equations of the physical problem and, subsequently, the estimation of their values based on the fitting of simulation results to available experimental results. The necessary set of six parameters for the current model has been identified based on the experimental data of Smith *et al.* (1996). The fitting of simulation results to the experimental measurements is accomplished by the solution of a properly defined optimization problem.

2 FLASHING FUNDAMENTALS

The basic phenomenon of interest occurring in a TFC unit is the two-phase expansion, commonly referred to as flashing. Flashing occurs as a result of sudden depressurization of a liquid at high temperatures (the same phenomenon at low temperatures is called cavitation). The liquid depressurization incurs a phase change since a fraction of its mass is vaporized. This phase change is the result of a nucleation process, i.e. a localized formation of a distinct thermodynamic phase. Nucleation is divided into two categories, namely homogenous and heterogenous, and it occurs only if an interface is formed at the vapor-liquid boundaries. The phenomenon is accelerated by superheating the liquid, i.e. increasing its temperature above the saturation temperature corresponding to its pressure. The liquid superheat ΔT_{sh} has a maximum attainable value, beyond which phase change will take place, and it is acknowledged as the major accelerating force of nucleation, in combination with the preexisting nucleation sites in the liquid (Liao and Lucas, 2017). Superheating of a liquid is always caused by its sudden depressurization and it can be achieved through the following three different physical mechanisms:

- The dynamic pressure of a flowing liquid of high temperature may drop as a result of the increase in the flow area.

- A pressure drop of a liquid may occur because of cracks or safety valves opening in a pressurized vessel.
- Liquid superheating may be the result of the hydrostatic pressure drop in a vertical channel flow.

The challenge in simulating flashing flows is the modeling of the thermodynamic non-equilibrium between the liquid and vapor phases. Mechanical and thermal non-equilibrium exist simultaneously at the vapor-liquid interface. A common assumption when modeling flashing flows is that the two phases are in mechanical equilibrium, and, therefore, vapor is generated because of the thermal non-equilibrium alone (Liao and Lucas, 2017). In this case, a method for calculating the interfacial heat transfer, i.e. the heat transfer rate from the liquid to the vapor phase at their interface, is necessary. The commonly applied models in the literature for the calculation of the interfacial heat transfer are the Homogenous Relaxation Model (HRM) (Downar-Zapolski *et al.*, 1996), the Homogenous Equilibrium Model (HEM) (Yang *et al.*, 1986), the Bubble Growth Model (BGM) (Liao and Lucas, 2017), and the Interfacial Exchange Model (IEM) (Liao and Lucas, 2017).

3 MODELING

3.1 Assumptions

The developed model is a one-chamber thermodynamic model. At a given male rotor angle, which corresponds to a specific time interval from the onset of the working cycle, the volume of the working chamber is predefined according to the geometrical characteristics of the expander. In the current work, the variation of the working chamber volume relative to the rotation angle of the male rotor is an input from the manufacturer of the expander (Smith *et al.*, 1996). The variation of the volume of the working chamber is attributed to the expansion of the vapor phase, and leakages from the liquid phase are not taken into consideration.

The conservation equations are solved separately for the liquid and vapor phases between successive rotor angles in a formulation similar to that of a two-fluid model. The properties of the two phases are assumed uniform at the cross-sections of the expander and no spatial gradients are taken into account. Moreover, the problem is considered steady state. The conservation equations for the two phases are coupled by the interfacial heat transfer. The two phases are assumed to be in mechanical equilibrium, but thermal non-equilibrium, and the vapor phase remains saturated throughout the working cycle of the expander. During the expansion phase of the operation cycle, the heat losses towards the expander wall for both vapor and liquid phases are considered negligible.

3.2 Suction

The suction process is divided into two separate sub-processes which are assumed to take place in consecutive order. Initially, the working fluid undergoes an adiabatic supply pressure drop which is followed by isobaric cooling.

The adiabatic supply pressure drop is modeled as a fast and isentropic flow of a saturated mixture through a converging nozzle with a throat cross-sectional area equal to A_{in}. For low vapor qualities the mixture may be considered incompressible, and the supply pressure drop is calculated from the Bernoulli equation for the incompressible fluid

$$p_{ad} = p_{in} - \frac{v_{in}}{2}\left(\frac{\dot{m}_{in}}{A_{in}}\right)^2 \quad (1)$$

where p_{ad} and p_{in} are the pressure at the end of the process and the onset of suction, respectively. Moreover, v_{in} is the specific volume of the working fluid, and $\dot{m}_{in}$ is the mass flow rate of the working fluid at the end of the process. The energy conservation equation for the working fluid is

$$\dot{m}_{in} h_{in} = \dot{m}_{ad} h_{ad} \quad (2)$$

where h_{in} is the specific enthalpy of the saturated mixture at the onset of the suction process. Moreover, $\dot{m}_{ad}$ is the mass flow rate and h_{ad} is the specific enthalpy of the mixture at the end of the adiabatic process. For continuity reasons $\dot{m}_{ad} = \dot{m}_{in}$. The pressure drop induces a liquid superheat $\Delta T_{l,ad}$ above the saturation temperature at p_{ad} which is calculated by

$$h_{l,ad} = h_{l,sat,ad} + c_{p_{l,ad}} \Delta T_{l,ad} \quad (3)$$

In the above formula, $h_{l,ad}$ and $h_{l,sat,ad}$ are the specific enthalpies of the superheated and saturated liquid at p_{ad}, and $c_{p_{l,ad}}$ is the specific heat under constant pressure of the liquid at p_{ad}.
Following the pressure drop, the isobaric cooling process of the working fluid at p_{ad} takes place. Assuming that T_w is a uniform temperature of a fictitious metal envelope representing the mass of the expander shell and the rotating lobes (Lemort *et al.*, 2009), the heat losses rate $\dot{q}_{l,in}$ of the liquid phase during the cooling process is equal to

$$\dot{q}_{l,in} = AU_{l,in}\left(T_{l,ad} - T_w\right) \tag{4}$$

where $T_{l,ad}$ is the temperature of the liquid before cooling, and $AU_{l,in}$ is the overall heat transfer coefficient between the liquid and the expander wall. The energy equation balance of the liquid during this process is

$$\dot{m}_{l,ad} h_{l,ad} = \dot{m}_{l,ex} h_{l,ex} + \dot{q}_{l,in} \tag{5}$$

where $\dot{m}_{l,ex} = \dot{m}_{l,ad}$ is the mass flow rate and $h_{l,ex}$ is the specific enthalpy of the liquid at the end of the suction process. For a low vapor quality of the saturated mixture feeding the expander, the heat losses from the vapor phase are not considered in the cooling phase of the suction process.

3.3 Expansion

The primary characteristic of the two-phase expansion is that the vapor mass constantly varies throughout the depressurization process. Therefore, the prediction of the evolution of vapor mass is a crucial aspect in the modeling of the phenomenon. In the present work, this is accomplished by dividing the expansion chamber into sub-chambers. If the expansion chamber is sub-divided into N sub-chambers, $N+1$ control points will be created. The first control point in the expansion chamber corresponds to the end of the suction process where the thermodynamic properties of the two-phase mixture have been already defined. An intermediate sub-chamber i is defined by the control points i and $i+1$. The control points correspond to different values of the male rotor angle. The conservation equations are applied for both phases separately at every sub-chamber. The following physical phenomena are considered to occur successively in a sub-chamber:

1. Vapor mass is generated by interfacial heat transfer between the superheated liquid and the saturated vapor at control point i. For the calculation of the interfacial heat transfer rate the IEM is applied, i.e. the vapor generation rate is governed by an overall heat transfer coefficient between the liquid and vapor phases.
2. A fraction of the total vapor mass escapes the expansion process through the available leakage paths.
3. The remaining vapor mass expands until control point $i+1$ resulting in further depressurization.

At control point i, the pressure of the two-phase mixture is p_i. The temperature $T_{g,i}$ of the vapor phase is equal to the saturation temperature at p_i. In the general case, the temperature $T_{l,i}$ of the liquid phase will not be equal to the saturation temperature. The liquid superheat $\Delta T_{l,i}$ is equal to:

$$\Delta T_{l,i} = T_{l,i} - T_{g,i} \tag{6}$$

The available liquid superheat is the driving force for the phase change. The vapor mass flow rate $\delta\dot{m}_{g,i}$ to be generated is

$$\delta\dot{m}_{g,i} = \frac{AU_{int,i}\Delta T_{l,i}}{h_{lg}(p_i)} \tag{7}$$

where $AU_{int,i}$ and $h_{lg}(p_i)$ stand for the overall interfacial heat transfer coefficient between the two phases and the enthalpy of vaporization at p_i, respectively. The total mass flow rate $\dot{m}_{g,pc,i}$ of the vapor phase post vaporization is

$$\dot{m}_{g,pc,i} = \dot{m}_{g,i} + \delta\dot{m}_{g,i} \tag{8}$$

whereas the total mass flow rate of the liquid is

$$\dot{m}_{l,pc,i} = \dot{m}_{l,i} - \delta\dot{m}_{g,i} \tag{9}$$

In Equations (8) and (9) $\dot{m}_{g,i}$ and $\dot{m}_{l,i}$ are the mass flow rates of the vapor and liquid phase at control point i, respectively. These flow rates, as well as all the thermodynamic properties of the mixture, have already been calculated from the mass and energy balance at sub-chamber $i-1$. The energy balance equation for the liquid phase for the vaporization process is

$$\dot{m}_{l,i}h_{l,i} = \dot{m}_{l,pc,i}h_{l,pc,i} + \delta\dot{m}_{g,i}h_{g,i} \quad (10)$$

In the above equation $h_{l,i}$, $h_{l,pc,i}$, and $h_{g,i}$ represent the specific enthalpies of the liquid before vaporization takes place, of the liquid after vaporization has finished, and of the saturated vapor at p_i, respectively.

Leakage flows occur in a twin-screw expander through the inter-lobe, rotor tip-expander shell, and blowhole clearances. The typical approach in modeling leakage flows, i.e. flow through orifices, has been applied in this work also. All the above-mentioned leakage paths are grouped into a fictitious flow path through a convergent nozzle of throat cross-sectional area equal to $A_{g,leak}$. The flow through the nozzle is treated as isentropic and vapor as an ideal gas. The vapor mass flow rate $\dot{m}_{g,leak,i}$ at the nozzle throat is

$$\dot{m}_{g,leak,i} = \frac{A_{g,leak}}{v_{g,thr,i}}\sqrt{2\left(h_{g,i} - h_{g,thr,i}\right)} \quad (11)$$

where $v_{g,thr,i}$ and $h_{g,thr,i}$ are the specific volume and enthalpy at the nozzle throat. The values of $v_{g,thr,i}$ and $h_{g,thr,i}$ are a function of the pressure $p_{thr,i}$ at the nozzle throat. The value of $p_{thr,i}$ is:

$$p_{thr,i} = \max\left(p_{dis}, p_{crit,i}\right) \quad (12)$$

In the above expression, p_{dis} is the discharge pressure and $p_{crit,i}$ is the critical pressure at the nozzle throat. The mass flow rate $\dot{m}_{g,ex,i}$ remaining in the expansion chamber is now

$$\dot{m}_{g,ex,i} = \dot{m}_{g,pc,i} - \dot{m}_{g,leak,i} \quad (13)$$

and this vapor mass is to be expanded. The energy balance for the expanding vapor phase is given by

$$\dot{m}_{g,ex,i}h_{g,i} = \dot{m}_{g,ex,i}h_{g,i+1} + \dot{w}_i \quad (14)$$

In Equation (14) $h_{g,i+1}$ is the specific enthalpy of the saturated vapor at p_{i+1} and $\dot{w}_i$ is the thermodynamic work supplied to the rotors during expansion. On the other hand, the energy balance for the liquid phase during the expansion of the vapor phase is given by

$$\dot{m}_{l,pc,i}h_{l,pc,i} = \dot{m}_{l,pc,i}h_{l,i+1} \quad (15)$$

The specific enthalpy $h_{l,i+1}$ of the liquid and the corresponding superheat $\Delta T_{l,i+1}$ at p_{i+1} may now be calculated from Equation (15).

3.4 Discharge

At the end of the expansion process, the pressure of the two-phase mixture is equal to $p_{ex,out}$. The vapor and liquid mass flow rates are $\dot{m}_{g,exout}$ and $\dot{m}_{l,exout}$, respectively. The vapor mass $\dot{m}_{g,exout}$ is mixed with the vapor leakages flows calculated throughout the expansion process. Therefore, the total mass flow rate $\dot{m}_{g,dis}$ to be discharged is

$$\dot{m}_{g,dis} = \dot{m}_{g,exout} + \sum_{i=1}^{N}\dot{m}_{g,leak,i} \quad (16)$$

The pressure of the mixture is assumed to be equal to the discharge pressure p_{dis}. The heat losses rate $\dot{q}_{g,dis}$ from the vapor at the discharge port are calculated by the formula

$$\dot{q}_{g,dis} = AU_{g,dis}\left(T_{g,exout} - T_w\right) \quad (17)$$

In Equation (17) $AU_{g,dis}$ and $T_{g,exout}$ are the overall heat transfer coefficient between the vapor and the expander wall and the temperature of the vapor mixture, respectively. The specific enthalpy $h_{g,dis}$ of the discharged by the expander vapor mixture is calculated from the vapor energy balance at the discharge port

$$\dot{m}_{g,dis}h_{g,exout} = \dot{m}_{g,dis}h_{g,dis} + \dot{q}_{g,dis} \quad (18)$$

where $h_{g,exout}$ is the specific enthalpy of the vapor mixture at the onset of the discharge process. Similar to the vapor phase, the heat losses rate $\dot{q}_{l,dis}$ from the liquid phase at the discharge port is

$$\dot{q}_{l,dis} = AU_{l,dis}\left(T_{l,exout} - T_w\right) \quad (19)$$

In the above formula, $AU_{l,dis}$ is the overall heat transfer coefficient between the liquid and the expander wall at the discharge port. The temperature $T_{l,exout}$ of the liquid is equal to its temperature at the end of the expansion process. Having calculated the heat rate losses $\dot{q}_{l,dis}$, the energy balance equation for the liquid at the discharge port is

$$\dot{m}_{l,exout}h_{l,exout} = \dot{m}_{l,exout}h_{l,dis} + \dot{q}_{l,dis} \quad (20)$$

The above formula leads to the calculation of the specific enthalpy $h_{l,dis}$ of the discharged liquid, given that $h_{l,exout}$ is the specific enthalpy of the liquid at the end of the expansion process.

3.5 Heat balance over the expander

The total heat losses from the expander wall towards the ambient are calculated by the equation:

$$\dot{q}_{amb} = AU_{amb}(T_w - T_{amb}) \tag{21}$$

In Equation (21) AU_{amb} is the overall heat transfer coefficient from the expander casing towards the environment, and T_{amb} is the ambient temperature. The heat balance over the expander is expressed by

$$\dot{q}_{amb} = \dot{q}_{l,in} + \dot{q}_{l,dis} + \dot{q}_{g,dis} + \dot{w}_{loss} \tag{22}$$

From the combination of Equations (21) and (22) the temperature T_w of the expander wall is calculated. The term $\dot{w}_{loss}$ in Equation (22) represents all the mechanical losses (friction losses and losses in the bearings) during the operation of the expander. These losses are difficult to quantify in the absence of direct shaft power measurements. In the present work $\dot{w}_{loss}$ is assumed to be a percentage, in the order of 2-3%, of the total work derived from the indicator diagrams.

4 RESULTS AND DISCUSSION

4.1 Model parameters & optimization process

The two-phase expansion numerical model was developed in the Engineering Equations Solver (EES) (v10.834) software suite. As already mentioned, the model development was based on the experimental data of Smith *et al.* (1996). The variation of the working chamber volume relative to the male rotor angle is an input for the model. The displacement volume of the expander under investigation is 2.7×10^{-4} m^3, whereas its built-in volume ratio is 3. In all experiments the working fluid was R113.

The optimization process was performed in EES by applying a genetic algorithm integrated into the software package. Based on the previously presented governing equations, a set of six parameters has been identified. The values of the parameters were calculated by minimizing the objective function f_{opt}, which is calculated by

$$f_{opt} = \sum_{j=1}^{N_s} \left[f_{su} \left(\frac{abs(p_{ad,exp} - p_{ad,sim})}{p_{ad,exp}} \right) + f_{ex} \sum_{i=2}^{N+1} \left(\frac{abs(p_{i,exp} - p_{i,sim})}{p_{i,exp}} \right) \right] \tag{23}$$

In the above formula, the index j runs through all the available experimental data sets. The subscripts exp and sim represent experimental and numerical data, respectively. The first and second terms in the bracket weigh the influence of the suction and expansion phases of the working cycle, respectively. The values $p_{i,exp}$ and $p_{i,sim}$ are the pressure values at control point i, respectively. For the given set of experimental data, a sensitivity analysis indicated that a total of 12 sub-chambers in the expansion process was adequate to obtain a sub-chamber number independent solution. The values of the weighting factors f_{su} and f_{ex} are equal to 0.5 and they have been determined based on an initial calibration procedure of the optimization module. The parameters, along with their description, units in SI, symbols, and calculated values from the optimization algorithm are listed in Table 1.

Table 1: List of parameters for the empirical low-order model.

Parameter	Symbol	Value	Units
Nozzle throat cross-sectional area at suction	A_{in}	7.78×10^{-4}	m^2
Overall heat transfer coefficient from liquid to expander wall at suction	$AU_{l,in}$	863.10	W/K
Nozzle throat cross-sectional area for vapor leakages flow during expansion	$A_{g,leak}$	1.10×10^{-4}	m^2
Overall heat transfer coefficient from liquid to expander wall at discharge	$AU_{l,dis}$	94.58	W/K
Overall heat transfer coefficient from vapor to expander wall at discharge	$AU_{g,dis}$	94.05	W/K

Overall heat transfer coefficient from expander wall to the ambient	AU_{amb}	829.60	W/K

Concerning the interfacial heat transfer coefficients $AU_{int,i}$, it must be mentioned that, initially, they were included in the optimization process. However, it was observed that their optimized values fit very well to the values which would be calculated by application of the empirical formula of Miyatake *et al.* (2001)

$$\eta_f = \begin{cases} 1 - [1 + 2.5(\Delta T - 1)]^{-1}, \Delta T > 1 \\ 0, \Delta T < 1 \end{cases} \quad (24)$$

Therefore, the calculation of $AU_{int,i}$ has not been included in the optimization process. Equation (24) is valid for pure substances and correlates the flashing efficiency η_f with the locally available liquid superheat ΔT for a pure substance. The flashing efficiency η_f is a measure of the deviation of a phase change process from the ideal process which would result in thermal equilibrium between phases. It must be noted that the interfacial heat transfer coefficients $AU_{int,i}$ may be easily included in the optimization process, which may be necessary for other types of expanders.

4.2 Simulations

The target of the numerical experiments presented in this section is to assess the reliability of the developed model for the simulation of the two-phase expansion. For this purpose, the numerical tool, with the optimized values of the parameters, is operated with boundary conditions identical to the experiments.

The boundary conditions for the simulations are the pressure p_{in} and quality x_{in} of the saturated mixture at the onset of suction, the discharge pressure p_{dis}, the rotational speed n_{rot} of the expander, and the ambient temperature T_{amb}. The outputs of the model are the mass flow rate $\dot{m}_{in}$ through the expander, the values of pressure along the working chamber, and the temperature T_w of the expander wall. The boundary conditions for the performed simulations along with the calculated values for $\dot{m}_{in}$ and T_w are listed in Table 2.

The evolution of the simulated and experimentally measured pressure relative to the chamber volume for the expansion process and rotational speeds equal to 2400, 3600, and 4800 rpm and inlet pressure p_{in} equal to 4.20 bar is presented in Figure 1. A very good fit between the simulation results and the experimental data is observed. A deviation is observed at the end of the expansion process when over-expansion occurs (n_{rot} equal to 3600 and 4800 rpm). This is attributed to the fact that in the case of over-expansion a backflow from the discharge port towards the expansion chamber takes place.

Table 2: Boundary conditions and output data from two-phase expansion simulations.

Boundary conditions					**Output data**	
p_{in} **(bar)**	p_{dis} **(bar)**	n_{rot} **(rpm)**	x_{in} **(-)**	T_{amb} **(°C)**	$\dot{m}_{in}$ **(kg/s)**	T_w **(°C)**
4.20	1.90	2400	0.02	20	10.15	57.65
4.20	2.00	3600	0.04	20	7.79	60.45
4.20	1.70	4800	0.08	20	6.29	63.35

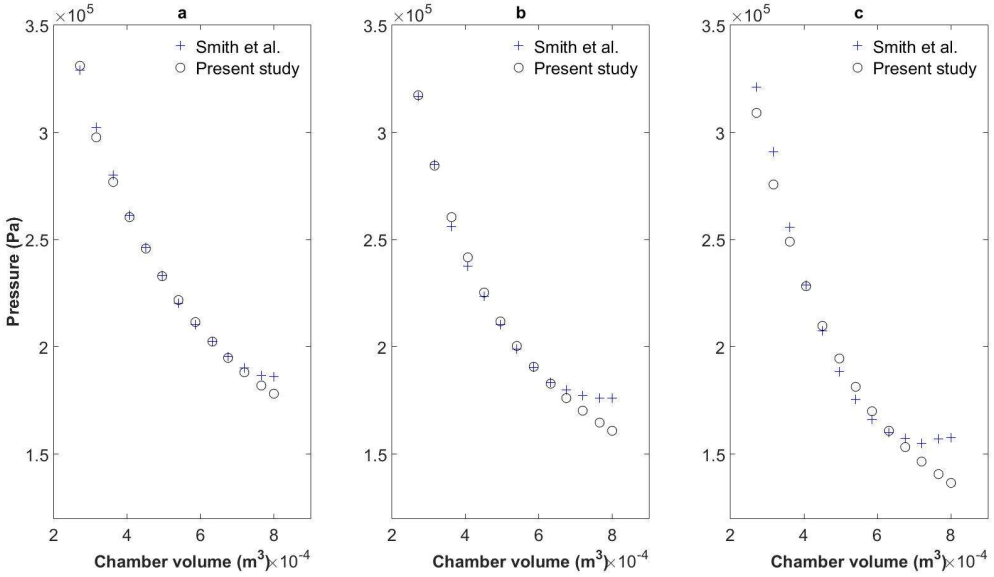

Figure 1: Pressure vs expansion chamber volume. P_{in}=4.20 bar, a) n_{rot}=2400 rpm, b) n_{rot}=3600 rpm, and c) n_{rot}=4800 rpm

Concerning the performance of the examined expander, the indicated power $P_{ind,c}$ produced by the working chamber is calculated by

$$P_{ind,c}=\frac{n_{rot}}{60}\int VdP \tag{25}$$

whereas the adiabatic efficiency η_{ad} of the expander is

$$\eta_{ad}=\frac{P_{ind,c}}{\dot{m}_{in}\left(h_{in}-h_{out,is}\right)} \tag{26}$$

In Equation (25) $h_{out,is}$ is the specific enthalpy corresponding to the isentropic expansion of the saturated mixture from the inlet pressure p_{in} to the discharge pressure p_{dis}. The calculated performance parameters of the expander for the simulated cases are listed in Table 3.

Table 3: Calculated performance parameters of the expander.

n_{rot} (rpm)	$P_{ind,c}$ (W)	η_{ad}
2400	2795	0.179
3600	4208	0.323
4800	6235	0.363

The calculated values for the adiabatic efficiency comply with the conclusions from the experiments. Indeed, for low vapor qualities at the suction port, the adiabatic efficiency of the two-phase expander is not satisfactory. High adiabatic efficiencies have been obtained experimentally by increasing the vapor quality of the saturated mixture feeding the expander. This seems to be the most challenging issue for the implementation of the TFC. Different configurations of the TFC or development of expanders specifically designed for two-phase expansion may provide the basis for wide scale application of the TFC.

5 CONCLUSIONS

A semi-empirical thermodynamic low-order model for the simulation of two-phase expansion in twin-screw expanders was developed. A set of only six parameters was proven to be adequate for accurate simulations of the evolution of the working chamber pressure during the operation of the expander. The robustness of the model will be enhanced by incorporating more experimental data into the optimization algorithm.

The proposed methodology may be applied to other types of volumetric expanders, such as scroll and piston. Minor modifications are anticipated to be necessary for the scroll expander since the physical phenomena and their sequence during its operation are essentially the same. In the case of piston expanders, the same modeling philosophy may be applied, however special attention must be paid to the different nature of the suction and discharge phase of the operation cycle, and the absence of leakage flows. In any case, if experimental data are available for a volumetric expander the developed model may be adjusted to the specific type.

In the present work, R113 was the working fluid of the TFC cycle for all simulations. This choice was made to comply with the performed experiments on the specific expander. Expansion simulations for state of the art working fluids will be performed, provided that relevant experimental data become available. Simulations with other working fluids without a background of relevant experiments may be used for primary evaluation purposes, and it is expected that the accuracy of the results will increase as the thermophysical properties of the selected fluid approach the ones of the working fluid for which the model was originally developed.

The outcome of this work will be the development of a general, reliable, and computationally efficient tool that will be able to provide accurate results for the performance of a two-phase expander integrated into a TFC unit. As a result, the evaluation of the overall efficiency of a TFC unit will be more reliable compared to standard practice in the literature, wherein typical values for the isentropic efficiency of a two-phase expander are applied. Finally, it is anticipated that the processing of the numerical results will indicate possible modifications in the design of an expander to improve its adiabatic efficiency.

REFERENCES

Bianchi, G., Kennedy, S., Zaher, O., Tassou, S.A., Miller, J., Jouhara, H., 2018, Numerical modelling of a two-phase twin-screw expander for Trilateral Flash Cycle applications, *Int J Refrig*., vol. 88: p. 248-259.

Bianchi, G., Marchionni, M., Miller, J., Tassou, S.A., 2020, Modelling and off-design performance optimisation of a trilateral flash cycle system using two-phase twin-screw expanders with variable built-in volume ratio, *Appl Therm Eng*., vol. 179, 115671.

Downar-Zapolski, P., Bilicki, Z., Bolle, L., Franco, J., 1996, The non-equilibrium relaxation model for one-dimensional flashing liquid flow, *Int J Multiph Flow*, vol. 22, p. 473–483.

Iglesias Garcia, S., Ferreiro Garcia, R., Carbia Carril, J., Iglesias Garcia, D., 2018, A review of thermodynamic cycles used in low temperature recovery systems over the last two years, *Renew Sustain Energy Rev*., vol. 81, p. 760-767.

Kanno, H., Shikazono, N., 2015, Experimental and modeling study on adiabatic two-phase expansion in a cylinder, *Int J Heat Mass Transf*., vol. 86, p. 755-763.

Kliem B., 2005, Grundlagen des Zweiphasen-Schraubenmotors Fundamentals of the Two-Phase Screw-Type Engine. *Auslegung A Grad J Philos*.

Lecompte, S., Huisseune, H., van den Broek, M., De Paepe, M., 2015, Methodical thermodynamic analysis and regression models of organic Rankine cycle architectures for waste heat recovery, *Energy*, vol. 87. p. 60-76.

Lemort, V., Quoilin, S., Cuevas, C., Lebrun, J., 2009, Testing and modeling a scroll expander integrated into an Organic Rankine Cycle, *Appl Therm Eng*., vol. 29, p. 3094-3102.

Liao, Y., Lucas, D., 2017, Computational modelling of flash boiling flows: A literature survey, *Int J Heat Mass Transf*, vol. 111, p. 246–265.

Mckay, R.A., Sprankle, R.S., 1970, Helical Rotary Screw Expander, *Published online*.

Miyatake, O., Koito, Y., Tagawa, K., Maruta, Y., 2001, Transient characteristics and performance of a novel desalination system based on heat storage and spray flashing, *Desalination*, vol. 137, p. 157-166.

Öhman, H., Lundqvist, P., 2013, Experimental investigation of a Lysholm Turbine operating with superheated, saturated and 2-phase inlet conditions, *Applied Thermal Engineering*, vol 50, p. 1211-1218.

Smith, I.K., Stošić, N., Aldis, C.A., 1996, Development of the trilateral flash cycle system. Part 3: The design of high-efficiency two-phase screw expanders, *Proc Inst Mech Eng Part A J Power Energy*, vol210, no.1, p. 75-92.

Steidel, R.F., Miki, S., Flower, J.E., 1982, Performance characteristics of the lysholm engine as tested for geothermal power applications in the imperial valley, *J Eng Gas Turbines Power*, vol. 104, no. 1, p. 231-240.

Taniguchi, H., Kudo, K., Giedt, W.H., Park, I., Kumazawa, S., 1988, Analytical and experimental investigation of two-phase flow screw expanders for power generation, *J Eng Gas Turbines Power*, vol. 110, no. 4, p. 628-635.

Vasuthevan, H., Brümmer, A., 2017, Theoretical investigation of flash vaporisation in a screw expander, *Institute of Physics Publishing,* vol. 232.

Yang, J., Jones, O. C., Shin, T. S., 1986, Critical flow of initially subcooled flashing liquids: Limitations in the homogeneous equilibrium model, *Nucl Eng Des*, vol. 95, p. 197–206.

ACKNOWLEDGEMENT

The research work was supported by the Hellenic Foundation for Research and Innovation (H.F.R.I.) under the "First Call for H.F.R.I. Research Projects to support Faculty members and Researchers and the procurement of high-cost research equipment grant" (Project Number: 1087, Acronym: SOL-art).